Xiong *et al.*
Chinese Journal of Mechanical Engineering (2024) 37:36
https://doi.org/10.1186/s10033-024-01024-6

Chinese Journal of Mechanical Engineering

ORIGINAL ARTICLE

Open Access

Electrothermal Model Based Remaining Charging Time Prediction of Lithium-Ion Batteries against Wide Temperature Range

Rui Xiong[1*], Zian Zhao[1], Cheng Chen[1], Xinggang Li[1] and Weixiang Shen[2]

Abstract

Battery remaining charging time (RCT) prediction can facilitate charging management and alleviate mileage anxiety for electric vehicles (EVs). Also, it is of great significance to improve EV users' experience. However, the RCT for a lithium-ion battery pack in EVs changes with temperature and other battery parameters. This study proposes an electrothermal model-based method to accurately predict battery RCT. Firstly, a characteristic battery cell is adopted to represent the battery pack, thus an equivalent circuit model (ECM) of the characteristic battery cell is established to describe the electrical behaviors of a battery pack. Secondly, an equivalent thermal model (ETM) of the battery pack is developed by considering the influence of ambient temperature, thermal management, and battery connectors in the battery pack to calculate the temperature which is then fed back to the ECM to realize electrothermal coupling. Finally, the RCT prediction method is proposed based on the electrothermal model and validated in the wide temperature range from − 20 ℃ to 45 ℃. The experimental results show that the prediction error of the RCT in the whole temperature range is less than 1.5%.

Keywords Electric vehicles, Lithium-ion batteries, Remaining charging time, Electrothermal model

1 Introduction

The promotion of electric vehicles (EVs) is an important way to achieve the dual goals of "carbon peaking" and "carbon neutrality". Compared with fuel vehicles, EVs have the problems of short full mileage per charge or mileage anxiety, long charging time, and fuzzy prediction of remaining charging time (RCT). They have been hindering their adoption and popularization [1]. To solve these problems, many researchers focus on real-time optimization of EV charging in terms of EV charging state prediction [2–4] and optimization of EV charging strategy [5–7]. However, the accurate prediction of the RCT is the main basis for the real-time optimization of EV charging. Furthermore, the accurate prediction of the RCT also has the following significances [8]: (1) it is useful for users to plan and arrange their trips [9], (2) it is convenient for users to optimize their EV charging habits (e.g., select appropriate charging methods and extend the service life of EV batteries) [10], and (3) it is convenient for developers to optimize charging strategies [11, 12].

Although the accurate prediction of the RCT has important research value and commercial value, the research on the RCT is limited. Most of the algorithms to predict the RCT are based on a single cell under a narrow temperature range, they are difficult to be applied in the actual EV applications. Shi et al. [13] proposed a charging prediction method for the constant current constant voltage (CCCV) charging protocol. In the CC phase, the current in the current profile is not always constant. At the beginning of charging, the average charging current rate is close to the historical charging rate; In the later

*Correspondence:
Rui Xiong
rxiong@bit.edu.cn
[1] School of Mechanical Engineering, Beijing Institute of Technology, Beijing 100081, China
[2] School of Science, Computing and Engineering Technologies, Swinburne University of Technology, Hawthorn, VIC 3122, Australia

stage of charging, the average charging current rate is close to the current charging rate. Considering the confidence interval of historical charging data and real-time charging data, an online charging time estimation method is proposed to eliminate the error between demand current and actual current; In the CV stage, the radial basis function neural network is used to predict the battery resistance and charging current curve. Wu et al. [14] studied the charging time of the battery pack related to the temperature under the simple CCCV charging strategy to control the battery temperature within an appropriate range before the start of charging and did not pay attention to the temperature change within the charging period. In general, existing research on battery charging time faces the following problems:

(1) The research mainly focuses on the CCCV charging protocol of a battery, which is different from the fast-charging protocol in current commercial EVs.
(2) The research ignores the temperature change in the charging process, which leads to inaccurate charging time prediction for current commercial EVs.
(3) The research only targets the small range of battery operation temperature, which cannot be used for batteries against wide temperature range due to the popularization of EVs.

The battery temperature and charging current measured by a battery management system (BMS) in a commercial EVs during fast charging at − 4 ℃ are shown in Figure 1.

As can be seen in the enlarged area (1), the charging current suddenly increases and decreases due to the increase of battery temperature and SOC during the progress of the charging process. The similar situation also occurs in the other areas such as (2) and (3). Therefore, in the actual use of commercial EVs we need to pay attention to a wide range of temperature changes of the battery in EVs to achieve an accurate prediction of the charging time [15].

In this study, we propose a prediction method for the remaining charging time (RCT) based on an electrothermal model [16, 17]. It can effectively predict the RCT of EVs against a wide temperature range. The main contributions of this paper can be summarized as follows.

First, an equivalent circuit model (ECM) is developed for the characteristic battery cell selected from a battery pack, which takes the temperature and SOC into account. It is used to describe the electrical characteristics of a battery pack. Second, an equivalent thermal circuit model of the battery pack is established to describe the

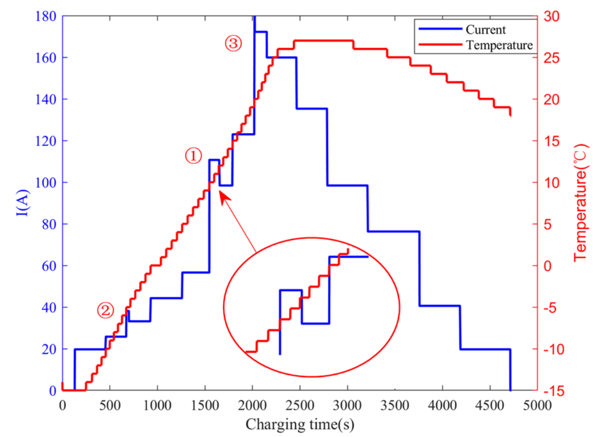

Figure 1 Temperature of the battery and the demand current at −4 ℃

temperature change of the battery pack. Third, establish an electrothermal model, and a prediction model for RCT is established based on the electrothermal model. Fourth, the model is validated against the wide temperature range of − 20 ℃ to 45 ℃ and the relative error of the RCT is less than 1.5%.

The remainder of this paper is organized as follows. Section 2 describes the development of the electrical model and equivalent thermal model. Section 3 establishes an electrothermal model and presents an RCT prediction method based on the model. Section 4 experimentally validates the proposed method at various temperatures. Conclusions are given in Section 5.

2 Electrical Model and Equivalent Thermal Model

2.1 Electrical Model

Due to the inconsistency of each battery cell of a battery pack, the "Buckets effect" (no matter how high a bucket is, the height at which it holds water depends on the lowest wooden board among them) often occurs in the use of the battery pack. A characteristic battery cell appropriately selected from a battery pack can be used to represent the battery pack [18]. For a battery pack, we monitor the voltage of each battery cell in the pack and use the battery cell with the highest voltage in the pack to protect the battery pack from overcharging during the charging process. Thus, we select the battery cell with the highest voltage as the characteristic battery cell and assume that all the other cells have the same characteristics as the characteristic battery cell. In such a way, an ECM for the characteristic battery cell is established to describe the characteristics of a battery pack. The ECM has the advantages of a few parameters, low calculation burden, and easy acquisition of battery characteristics. It is often used to describe the characteristics/behavior of the characteristic cell in commercial EVs. Therefore, the Thevenin model related to temperature and SOC is established to describe the characteristics of battery cell [19] as shown in Figure 2. According to Kirchhoff's law and the relationship between the capacitor voltage and its current, the state space equation of the circuit model can be expressed as:

$$\begin{cases} \dot{U}_{\mathrm{D}} = \dfrac{i_{\mathrm{L}}}{C_{\mathrm{D}}(T,SOC)} - \dfrac{U_{\mathrm{D}}}{R_{\mathrm{D}}(T,SOC)C_{\mathrm{D}}(T,SOC)}, \\ U_{\mathrm{t}} = U_{\mathrm{OCV}}(T,SOC) - U_{\mathrm{D}} - i_{\mathrm{L}}R_{\mathrm{i}}(T,SOC). \end{cases} \tag{1}$$

Thevenin model consists of three parts: voltage source U_{OCV}, ohmic internal resistance R_{i} and RC network. In addition, U_{D} denotes the polarization voltage of the battery during the dynamic process and U_{t} denote the terminal voltage. RC network describes the dynamic characteristics of a battery through a polarization internal resistance R_{D} and a polarization capacitor C_{D}.

Discretizing the polarization voltage in Eq. (1) leads to

$$\begin{aligned} U_{\mathrm{D}}(k+1) =& U_{\mathrm{D}}(k) \times e^{-\frac{1}{R_{\mathrm{D}}(k)C_{\mathrm{D}}(k)}} + i_{\mathrm{L},k} \\ & \times R_{\mathrm{D}}(k) \times (1 - e^{-\frac{1}{R_{\mathrm{D}}(k)C_{\mathrm{D}}(k)}}), \end{aligned} \tag{2}$$

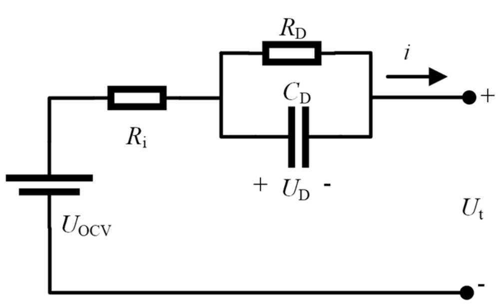

Figure 2 1-RC model related to temperature and SOC

where $R_{\mathrm{D}}(k)$, $C_{\mathrm{D}}(k)$ and $R_{\mathrm{i}}(k)$ are the model parameter at the kth time and their value is obtained through interpolation under different operating conditions.

The model parameters are modeled as a function of temperature and SOC. C_{D}, R_{D} and R_{i} are expressed as a polynomial related to battery temperature and SOC, and their specific relationships are obtained by HPPC experiments at different temperatures and SOC. Before testing, charge the tested unit to full charge, adjust the temperature to the specified temperature, load mixed pulse excitation in sequence, and then discharge for testing at different SOC at the same temperature. Using genetic algorithm for parameter identification, and the fitness function is the difference between the predicted terminal voltage and the actual terminal voltage. The predicted terminal voltage is obtained from the second equation of Eq. (1), where U_{OCV} is one of the identification parameters, and U_{D} is obtained from the calculation in Eq. (2). The calculation process of U_{D} involves the introduction of other identification parameters. Details of the parameters can be found in the Additional file 1. The image obtained is shown in Figure 3.

During the charging process, the ampere-hour integration method is used to calculate battery SOC:

$$SOC(k+1) = SOC(k) + \frac{\eta \times i_{\mathrm{L},k} \times \Delta t}{C_{\max}}, \tag{3}$$

where $SOC(k)$ is the SOC at the kth moment; η is the coulombic efficiency; $C_{\max}$ is the maximum available capacity.

2.2 Equivalent Thermal Model

There is the temperature inconsistency in a battery pack. To control the temperatures of all the battery cell in the pack within the safe range during charging process, we develop an equivalent thermal model (ETM) to reflect thermal behaviors of the battery pack at two extreme cases. First, when the battery pack is charged at high

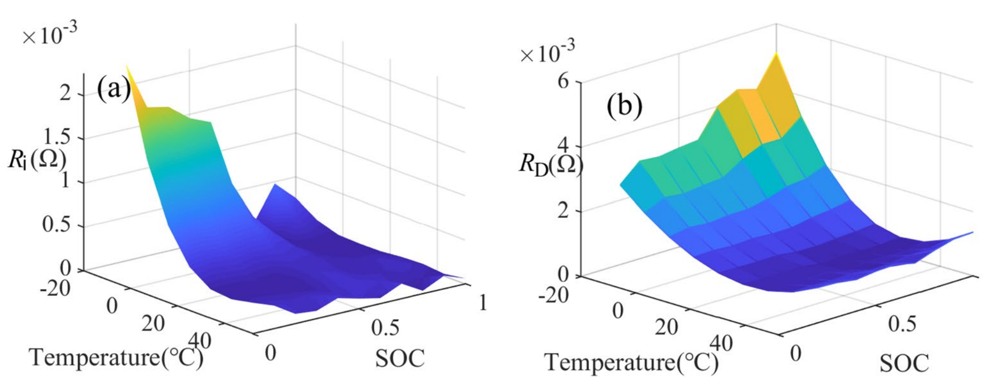

Figure 3 Identification results of (**a**) R_{i} and (**b**) R_{D}

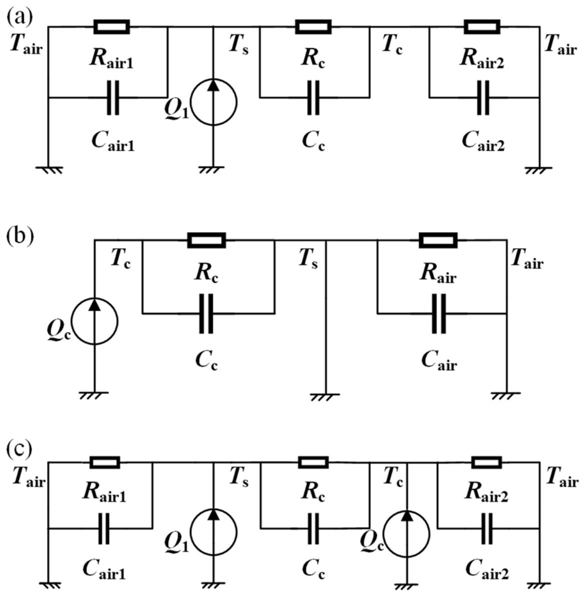

Figure 4 Equivalent thermal model: (**a**) Heating system only, (**b**) Charging only, (**c**) Heating system and charging

temperature (e.g., above 40 ℃) with high charge rate, battery temperature will rise rapidly and battery aging will accelerate. In this case, the high temperature battery cell in the pack will determine charging current. Second, when the battery pack is charged at low temperature (e.g., below 0 ℃) with high charge rate, severe lithium plating will occur in a battery cell. In this case, the low temperature battery cell in the pack will determine charging current. Based on the ECM, we obtain two groups of parameters of the ETM at both high temperature and low temperature to jointly control charging current [20, 21].

The battery pack shows different heat exchange conditions when the active thermal management system is involved or not. Due to the change of the heat transfer path, the heat exchange method and objects are changed [22, 23]. Therefore, the thermal model is divided into three cases: battery heating only, battery charging only and battery heating and charging, which is shown in Figure 4.

In Figure 4, Q_1 and Q_c are the liquid heating heat source and the battery charging excitation heat source, respectively; T_c, T_s and T_{air} are the battery temperature, the battery surface temperature and the ambient temperature; R_{air} and R_c are the thermal resistance of air and the internal thermal resistance of a battery; C_{air} and C_c are the heat capacity of air and the heat capacity of a battery.

The state equations of the three models are:

$$\begin{cases} C_{\text{cell}}\,\dot{T}_{\text{c}} + C_{\text{air1}}\,\dot{T}_{\text{c}} = Q_1 - \frac{T_{\text{c}}-T_{\text{s}}}{R_{\text{c}}} - \frac{T_{\text{c}}-T_{\text{air}}}{R_{\text{air1}}}, \\ C_{\text{air2}}\,\dot{T}_{\text{s}} = \frac{T_{\text{c}}-T_{\text{s}}}{R_{\text{c}}} - \frac{T_{\text{s}}-T_{\text{air}}}{R_{\text{air2}}}, \end{cases} \tag{4}$$

$$\begin{cases} C_{\text{cell}}\,\dot{T}_{\text{c}} = Q_{\text{c}} - \frac{T_{\text{c}}-T_{\text{s}}}{R_{\text{c}}}, \\ C_{\text{air}}\,\dot{T}_{\text{s}} = \frac{T_{\text{c}}-T_{\text{s}}}{R_{\text{c}}} - \frac{T_{\text{s}}-T_{\text{air}}}{R_{\text{air}}}, \end{cases} \tag{5}$$

$$\begin{cases} C_{\text{cell}}\,\dot{T}_{\text{c}} + C_{\text{air1}}\,\dot{T}_{\text{c}} = Q_1 - \frac{T_{\text{c}}-T_{\text{s}}}{R_{\text{c}}} - \frac{T_{\text{c}}-T_{\text{air}}}{R_{\text{air1}}}, \\ C_{\text{air2}}\,\dot{T}_{\text{s}} = Q_{\text{c}} + \frac{T_{\text{c}}-T_{\text{s}}}{R_{\text{c}}} - \frac{T_{\text{s}}-T_{\text{air}}}{R_{\text{air2}}}. \end{cases} \tag{6}$$

Taking battery heating and charging as an example, the offline process of the formula is as follows:

The state space Eq. (6) is transformed into the general expression as:

$$\begin{cases} \dot{x} = Ax + Bu, \\ y = Cx + Du, \end{cases}$$

$$\begin{cases} x = \left[\, T_{\text{c}} \;\; T_{\text{s}} \,\right]^{\text{T}}, \\ y = T_{\text{s}}, \\ u = \left[\, Q_1 \;\; T_{\text{air}} \;\; Q_{\text{c}} \,\right]^{\text{T}}, \end{cases}$$

$$\begin{cases} A = \begin{bmatrix} -\frac{R_{\text{air1}}+R_{\text{c}}}{(C_{\text{cell}}+C_{\text{air1}})R_{\text{air1}}R_{\text{c}}} & \frac{1}{(C_{\text{cell}}+C_{\text{air1}})R_{\text{c}}} \\ \frac{1}{C_{\text{air2}}R_{\text{c}}} & -\frac{R_{\text{air2}}+R_{\text{c}}}{C_{\text{air2}}R_{\text{air2}}R_{\text{c}}} \end{bmatrix}, \\ B = \begin{bmatrix} \frac{1}{C_{\text{cell}}+C_{\text{air1}}} & \frac{1}{(C_{\text{cell}}+C_{\text{air1}})R_{\text{air1}}} & 0 \\ 0 & \frac{1}{C_{\text{air2}}R_{\text{air2}}} & \frac{1}{C_{\text{air2}}} \end{bmatrix}, \\ C = \begin{bmatrix} 0 & 1 \end{bmatrix}, \\ D = \begin{bmatrix} 0 & 0 \end{bmatrix}. \end{cases} \tag{7}$$

Discreting Eq. (7) gives

$$x(k+1) = G(t)x(k) + H(t)u(k),$$
$$\begin{cases} G(t) = e^{At}, \\ H(t) = \int_0^t e^{At}\mathrm{d}t \cdot B, \end{cases} \tag{8}$$

where t is the sampling time length. Its Taylor expansion is

$$\begin{cases} G(t) = \begin{bmatrix} 1 - \frac{R_{\text{air1}}+R_{\text{c}}}{(C_{\text{cell}}+C_{\text{air1}})R_{\text{air1}}R_{\text{c}}}t & \frac{1}{(C_{\text{cell}}+C_{\text{air1}})R_{\text{c}}}t \\ \frac{1}{C_{\text{air2}}R_{\text{c}}}t & 1 - \frac{R_{\text{air2}}+R_{\text{c}}}{C_{\text{air2}}R_{\text{air2}}R_{\text{c}}}t \end{bmatrix}, \\ H(t) = \begin{bmatrix} t - \frac{R_{\text{air1}}+R_{\text{c}}}{2(C_{\text{cell}}+C_{\text{air1}})R_{\text{air1}}R_{\text{c}}}t^2 & \frac{1}{2(C_{\text{cell}}+C_{\text{air1}})R_{\text{c}}}t^2 \\ \frac{1}{2C_{\text{air2}}R_{\text{c}}}t^2 & T - \frac{R_{\text{air2}}+R_{\text{c}}}{2C_{\text{air2}}R_{\text{air2}}R_{\text{c}}}t^2 \end{bmatrix} \times \begin{bmatrix} \frac{1}{C_{\text{cell}}+C_{\text{air1}}} & \frac{1}{(C_{\text{cell}}+C_{\text{air1}})R_{\text{air1}}} & 0 \\ 0 & \frac{1}{C_{\text{air2}}R_{\text{air2}}} & \frac{1}{C_{\text{air2}}} \end{bmatrix}. \end{cases} \tag{9}$$

An offline database is established for parameter identification by using a genetic algorithm [24].

The heat source Q_1 is calculated by

$$Q_1 = WC(T_{\text{inlet}} - T_{\text{outlet}}), \tag{10}$$

where W is the liquid heating mass flow; C is the specific heat capacity of a heating liquid; T_{inlet} and T_{outlet} are the inlet water temperature and outlet water temperature [25].

Using the Bernardi heat generation model, we obtain the battery heat generation Q_c as

$$Q_c = (U_{\text{OCV}} - U_t)i_L + i_L T \frac{dU_{\text{OCV}}}{dT}. \tag{11}$$

Eq. (11) consists of two parts: ohmic heat generation and electrochemical reaction heat. The first term in the equation is ohmic heat generation; The second item is the heat of electrochemical reaction. $\frac{dU_{\text{OCV}}}{dT}$ is the entropy heat coefficient, used to calculate the heat of electrochemical reaction, whose values vary significantly under different SOC conditions. Calculate the entropy thermal coefficient of the battery by changing the battery temperature to obtain voltage at a fixed SOC. And its relationship with the SOC is shown in Figure 5 [26].

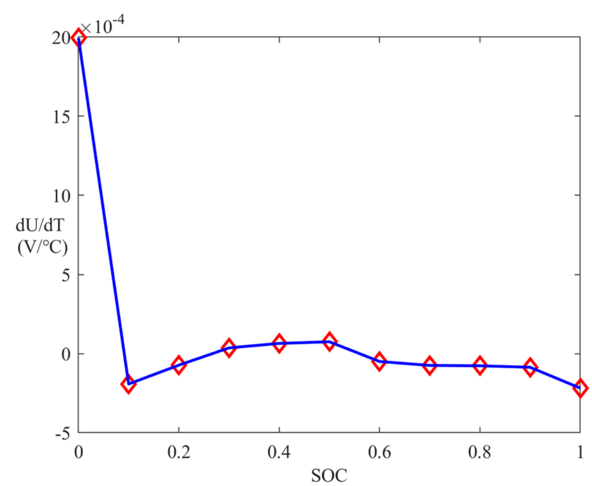

Figure 5 Obtaining entropy heat coefficient through experimental testing

The thermal model is also subjected to parameter identification through a genetic algorithm. In this case, the fitness function is the difference between the predicted battery temperature and the actual battery temperature. The predicted battery temperature is obtained from Eq. (8), where, during the process of predicting the battery temperature, all the thermal model identification parameters are introduced.

3 Electrothermal Model and Remaining Charging Time Prediction Method

By coupling the above-established ECM and ETM, we develop an electrothermal model [27]. Figure 6 shows the implementation of the electrothermal model. Step one, the battery initial charging current I_0, SOC_0 and temperature T_{cell} input to the ECM of the battery pack model based on the characteristic cell. Step two, the outputs of the ECM including battery terminal voltage U_t, OCV U_{OCV} and current I input into the ETM. Step three, the ETM calculates the maximum/minimum battery temperature T_{cell} at the next moment according to the results of the electrical model input. The heat of the equivalent thermal circuit model comes from two parts: the heat generation from the cell Q_c and the heat from the thermal management Q_t. Calculate the heat generation Q_c based on the input U_t, U_{OCV} and I. Calculate thermal management heat Q_t based on T_{cell} and thermal management strategy. Calculate the temperature of battery T_{cell} at the next moment based on the input ambient temperature

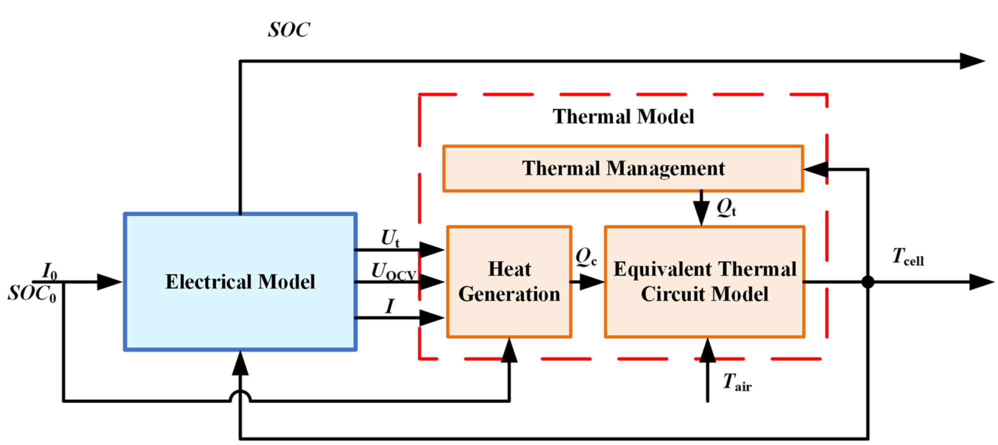

Figure 6 Implementation of electrothermal model

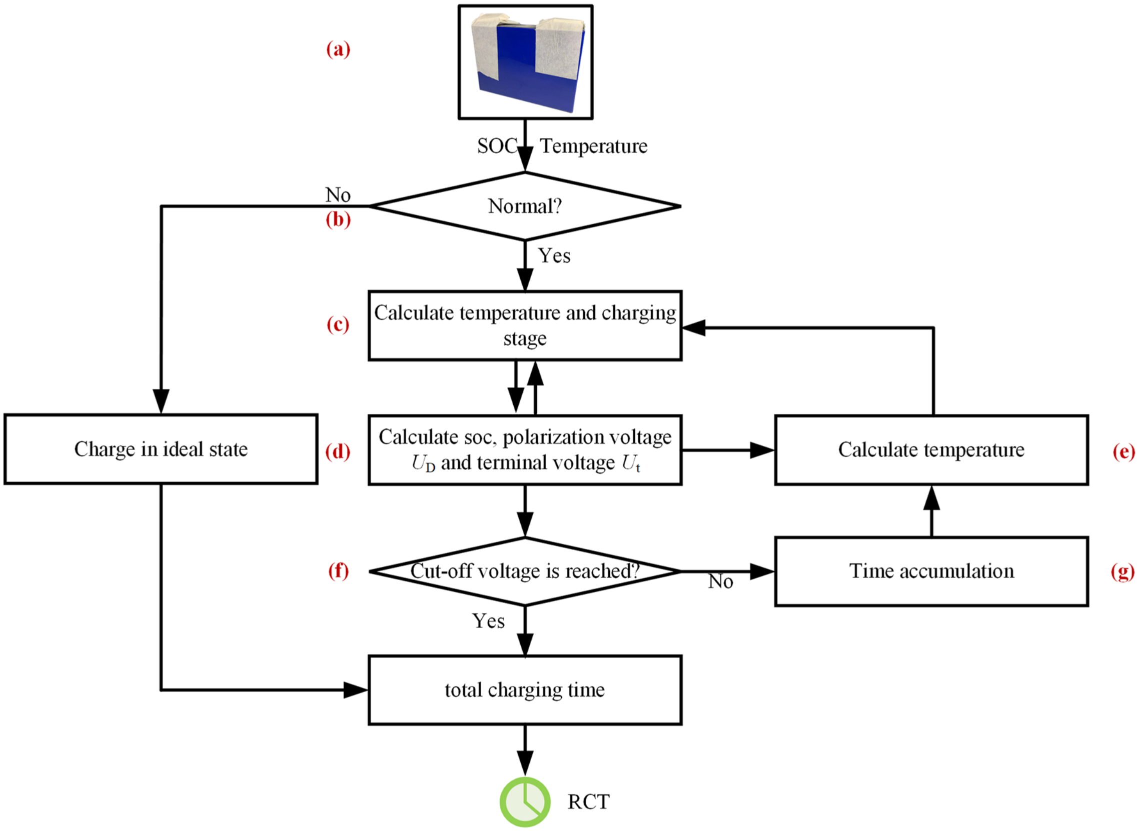

Figure 7 Process of RCT prediction

T_{air}, Q_c and Q_t. And returns the thermal model calculation results to the electrical model to realize the coupling of the electrical model and thermal model [28].

Based on the electrothermal model, the trajectory of battery charging is simulated for the RCT prediction [29, 30], where the prediction step is taken as 10 s. The process for RCT prediction is shown in Figure 7.

(a) Input temperature and SOC: Input initial temperature of battery T_{cell} and SOC into the model according to the information output by the battery module BMS.
(b) Whether it is an abnormal working condition: For the current less than 5A (because the charging equipment is under startup or startup failure condition), it is considered that an abnormal working condition occurs, and according to signals such as the SOC status sent out by BMS, following the ideal charging map and thermal management strategy (without considering the charging station charging rate), repeat steps c to g to calculate the ideal charging time.
(c) Calculation of temperature and charging stage: Commercial vehicles have two charging methods: high magnification multi-stage constant current (charging strategy varies with temperature and SOC) and low magnification constant current. Calculate the current charging stage according to the input temperature, SOC and selection of users charging station type (considering the charging station charging rate).
(d) Electrical model calculation: Calculate the electrical model parameters of the current stage.
(e) Thermal model calculation: When charging is not completed, calculate the battery temperature at end of the current step and feed it back to the electric model.
(f) Full charge judgment: Judge whether charging is completed.
(g) Time accumulation: The time is accumulated until the charging is completed.

Table 1 Specification of the battery cell

Items	Parameters
Materials	Lithium-Cobalt battery
Nominal capacity (A·h)	117
Voltage (V)	2.5–4.4
Temperature (℃)	−20~45

4 Validation

We verify the accuracy of the RCT prediction from three aspects (battery terminal voltage, temperature and charging time) with the temperature range from −20 ℃ to 45 ℃. The specification of the battery cell is shown in Table 1.

4.1 Battery Terminal Voltage

The experiments were carried out at − 17 ℃, 4 ℃, 8 ℃ and 45 ℃. The predicted and measured battery terminal voltage agree with each other very well, as shown in Figure 8; in this case, Figure 8(a) and (b) represent low-rate constant current charging experiments, while Figure 8(c) and (d) represent high-rate multi-stage constant current charging experiments. Therefore, in Figure 8(c) and (d), the voltage prediction errors exhibit larger fluctuations. However, most errors are within 20 mV. The initial voltage error is large because we set the initial value of the polarization voltage as 0 V, and the polarization voltage gradually converges and the error decreases in the recursion process.

4.2 Battery Temperature

The predicted and measured battery temperature agree each other very well too as shown in Figure 9 with most of the temperature prediction errors within 2 ℃. Because the accuracy of temperature sensor in the experiments was 1 ℃, the temperatures were shown in sawtooth shapes. Although the charging prediction process involves the accumulation of errors, thanks to the good consistency of the commercial battery system and the presence of battery system thermal management, there is no significant accumulation of errors in battery

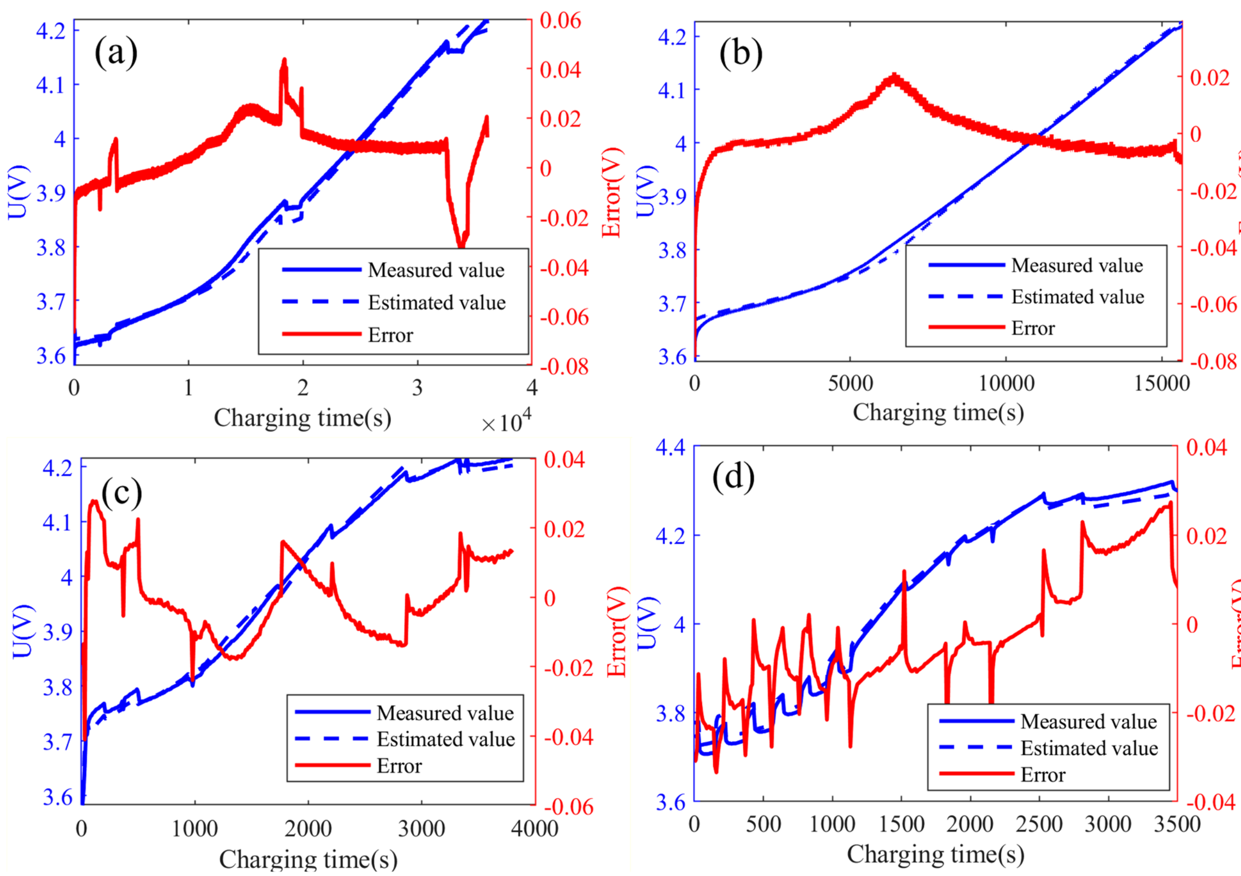

Figure 8 Voltage error profile of the ECM (**a**) −17 ℃, (**b**) 4 ℃, (**c**) 8 ℃, (**d**) 45 ℃

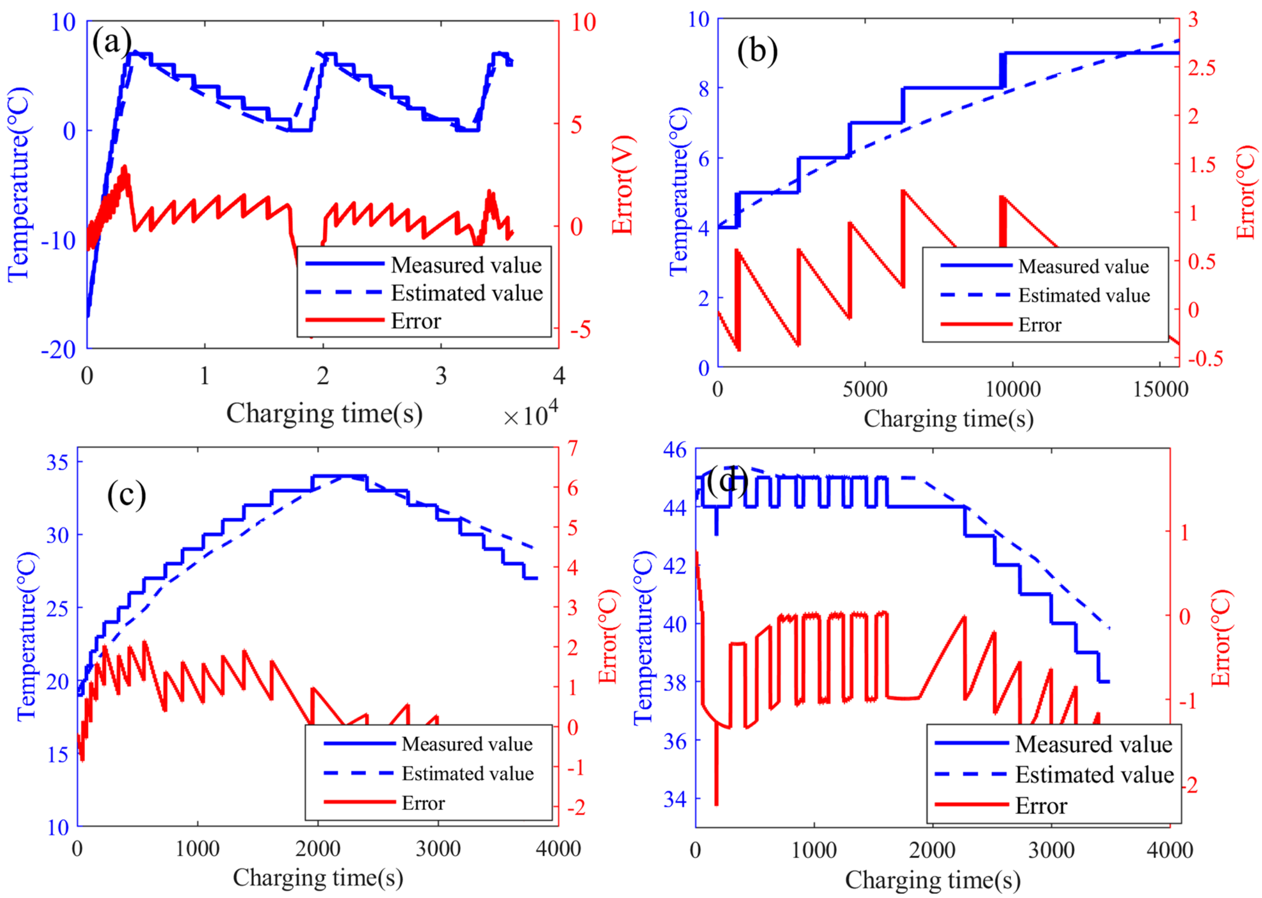

Figure 9 Temperature errors of the ETM at (**a**) −17 ℃, (**b**) 4 ℃, (**c**) 8 ℃, (**d**) 45 ℃

Table 2 Results of RCT predication

No.	T_{air} (℃)	*SOC*	*Time* (min)	$Time_{real}$ (min)	Δ*Error* (min)	δ*Error* (%)
1	7	50	48.5	49.1	0.6	1.22
2	-14.5	20.7	81.8	82.7	0.9	1.09
3	23.5	70	35.3	35	0.3	0.86
4	35.5	20	62.5	62.2	0.3	0.48
5	42.5	80	139	141	2	1.42
6	-19.5	80.4	78	78.4	0.4	0.51
7	5	40	219.1	219.8	0.7	0.32
8	26.5	7.1	339.9	340.7	0.8	0.23
9	-15.5	40.1	223	222.8	0.2	0.09
10	35.5	20	290.2	290.1	0.1	0.03

temperature prediction. Additionally, in this commercial electric vehicle model, the charging control temperature changes the charging rate every 5 ℃. Therefore, a temperature error of 2 ℃ fully satisfies the temperature accuracy requirements during the charging process of this vehicle.

4.3 Battery RCT

Under different temperatures and SOC, battery pack charging was carried out at different charging rates. The predicted and measured RCTs are shown in Table 2, where T_{air} is the ambient temperature; *SOC* is the initial

SOC when the charging starts; *Time* and $Time_{real}$ are the predicted time and the actual time; $\Delta Error$ and $\delta Error$ are the absolute error and relative error.

The results show that the electrothermal model developed in this study can accurately predict the RCT of the battery pack at different initial SOCs against wide temperature range because this model incorporates an ETM into an ECM to reflect thermal behaviors of the battery pack in real EV applications. Moreover, it can realize the charging time prediction of various commercial EVS charging strategies (i.e., multi-stage constant current fast charging such as Figure 8(c), (d), Figure 9(c), (d) and Table 2 No. 1–4; constant current low rate charging such as Figure 8(a), (b), Figure 9(a), (b) and Table 2 No. 5–10), and solve the current problem of charging time prediction against wide temperature range for battery packs with thermal management.

5 Conclusions

In this paper, a electrothermal model of a lithium-ion battery pack is established by coupling the ECM of the characteristic battery cell with the ETM of the battery pack, which is then used to develop a prediction model for the RCT during the charging process. The developed prediction model was tested in the ambient temperature range from − 20 ℃ to 45 ℃. The results show that the relative error of the RCT is less than 1.5%, the terminal voltage error is less than 20 mV and the temperature error is less than 2 ℃. These demonstrate that the prediction model can provide an accurate RCT against a wide temperature range which can meet the conditions of real EV applications. In the future, the influence of battery aging and battery pack inconsistency on the accuracy of the prediction model will be considered, and the online identification of the ETM parameters will be realized.

Supplementary Information

The online version contains supplementary material available at https://doi.org/10.1186/s10033-024-01024-6.

Additional file 1. C_D, R_D, R_i identification results at different SOC and temperatures.

Acknowledgements
Not applicable.

Author Contributions
RX conceptualization, supervision, writing—reviewing and editing the study; ZZ methodology, writing—original draft preparation; CC and W S review & editing, Supervision. All authors read and approved the final manuscript.

Funding
Supported by National Key R&D Program of China (Grant No. 2021YFB2402002) and Beijing Municipal Natural Science Foundation of China (Grant No. L223013).

Availability of Data and Materials
Not applicable.

Declarations

Competing Interests
The authors declare no competing financial interests.

Received: 4 May 2023 Revised: 4 January 2024 Accepted: 27 March 2024
Published online: 24 April 2024

References

[1] V Etacheri, R Marom, R Elazari, et al. Challenges in the development of advanced Li-ion batteries: A review. *Energy & Environmental Science*, 2011, 4(9): 3243-3262.
[2] C Zhang, T Amietszajew, S Li, et al. Real-time estimation of negative electrode potential and state of charge of lithium-ion battery based on a half-cell-level equivalent circuit model. *Journal of Energy Storage*, 2022, 51: 104362.
[3] A Maheshwari, S Nageswari. Real-time state of charge estimation for electric vehicle power batteries using optimized filter. *Energy*, 2022: 124328.
[4] B Çelikten, O Eren, Y Karataş. An execution time optimized state of charge estimation method for lithium-ion battery. *Journal of Energy Storage*, 2022, 51: 104307.
[5] Y Qin, P Zuo, X Chen, et al. An ultra-fast charging strategy for lithium-ion battery at low temperature without lithium plating. *Journal of Energy Chemistry*, 2022.
[6] R Xiong, B Zhu, K Zhang, et al. Design and implementation of a battery big data platform through intelligent connected electric vehicles. *Chinese Journal of Mechanical Engineering*, 2023, 36: 56.
[7] Y Li, K Li, Y Xie, et al. Optimization of charging strategy for lithium-ion battery packs based on complete battery pack model. *Journal of Energy Storage*, 2021, 37: 102466.
[8] R Xiong. Battery management algorithm for electric vehicles. 1st ed. Springer Singapore, 2020.
[9] F Guo, J Zhang, Z Huang, et al. Simultaneous charging station location-routing problem for electric vehicles: Effect of nonlinear partial charging and battery degradation. *Energy*, 2022, 250: 123724.
[10] J Huber, D Dann, C Weinhardt. Probabilistic forecasts of time and energy flexibility in battery electric vehicle charging. *Applied Energy*, 2020, 262: 114525.
[11] C Zhang, J Jiang, Y Gao, et al. Charging optimization in lithium-ion batteries based on temperature rise and charge time. *Applied Energy*, 2017, 194: 569-577.
[12] R Xiong, Y Sun, C Wang, et al. A data-driven method for extracting aging features to accurately predict the battery health. *Energy Storage Materials*, 2023.
[13] J Shi, M Tian, S Han, et al. Electric vehicle battery remaining charging time estimation considering charging accuracy and charging profile prediction. *Journal of Energy Storage*, 2022, 49: 104132.
[14] W Wu. Charging time estimation and study of charging behavior for automotive Li-ion battery cells using a Matlab/Simulink model. 2016.
[15] L He, H Jing, Y Zhang, et al. Review of thermal management system for battery electric vehicle. *Journal of Energy Storage*, 2023, 59: 106443.
[16] T Mesbahi, R Sugrañes, R Bakri, et al. Coupled electro-thermal modeling of lithium-ion batteries for electric vehicle application. *Journal of Energy Storage*, 2021, 35: 102260.
[17] J He, M S Hosen, R Youssef, et al. A lumped electro-thermal model for a battery module with a novel hybrid cooling system. *Applied Thermal Engineering*, 2023, 221: 119874.
[18] C Chen, R Xiong, R Yang, et al. A novel data-driven method for mining battery open-circuit voltage characterization. *Green Energy and Intelligent Transportation*, 2022, 1(1):8.
[19] X Hu, S Li, H Peng. A comparative study of equivalent circuit models for Li-ion batteries. *Journal of Power Sources*, 2012, 198: 359-367.

[20] Y Ma, Y Cui, H Mou, et al. Core temperature estimation of lithium-ion battery for EVs using Kalman filter. *Applied Thermal Engineering*, 2020, 168: 114816.
[21] M Steinhardt, J Barreras, H Ruan, et al. Me-ta-analysis of experimental results for heat capacity and thermal conductivity in lithium-ion batteries: A critical review. *Journal of Power Sources*, 2022, 522: 230829.
[22] R Yang, R Xiong, W Shen, et al. Extreme learning machine-based thermal model for lithium-ion batteries of electric vehicles under external short circuit. *Engineering*, 2021, 7(3): 395-405.
[23] Z Chen, B Zhang, R Xiong, et al. Electro-thermal coupling model of lithium-ion batteries under external short circuit. *Applied Energy*, 2021, 293: 116910.
[24] L Chen, M Hu, K Cao, et al. Core temperature estimation based on electro-thermal model of lithium-ion batteries. *International Journal of Energy Research*, 2020, 44(7): 5320-5333.
[25] S Chen, G Zhang, C Wu, et al. Multi-objective optimization design for a double-direction liquid heating system-based Cell-to-Chassis battery module. *International Journal of Heat and Mass Transfer*, 2022, 183: 122184.
[26] D Bernardi, E Pawlikowski, J Newman. A general energy balance for battery systems. *Journal of the Electrochemical Society*, 1985, 132(1): 5.
[27] R Xiong, Z Li, R Yang, et al. Fast self-heating battery with anti-aging awareness for freezing climates application. *Applied Energy*, 2022, 324: 119762.
[28] H Pang, L Guo, L Wu, et al. A novel extended Kalman filter-based battery internal and surface temperature estimation based on an improved electro-thermal model. *Journal of Energy Storage*, 2021, 41: 102854.
[29] Y Li, K Li, Y Xie, et al. Optimized charging of lithium-ion battery for electric vehicles: Adaptive multistage constant current–constant voltage charging strategy. *Renewable Energy*, 2020, 146: 2688-2699.
[30] W Wang, J Wang, J Tian, et al. Application of digital twin in smart battery management systems. *Chinese Journal of Mechanical Engineering*, 2021, 34: 57.

Rui Xiong born in 1985, graduated from *Beijing Institute of Technology, China* (Ph.D.), and now is a Professor at *National Engineering Research Center for Electric Vehicles, Beijing Institute of Technology, China*. His research interests include electrified vehicles, energy storage, batteries, and machine learning.

Zian Zhao born in 1999, is currently a master candidate at *National Engineering Research Center for Electric Vehicles, Beijing Institute of Technology, China*. His research interests include coordinated control of charging and heating in lithium-ion batteries, as well as charging optimization.

Cheng Chen born in 1992, is currently a postdoctoral researcher at *Advanced Energy Storage and Applications group, Beijing Institute of Technology, China*. His research interests include battery modeling, state estimation, and life prediction methods for new energy vehicle applications and hierarchical energy storage applications.

Xinggang Li born in 1994, is pursuing his PhD at *Advanced Energy Storage and Applications Group at Beijing Institute of Technology, China*. His research interests include battery temperature estimation and thermal safety management.

Weixiang Shen graduated from *University of Hong Kong, Hong Kong, China* (Ph.D.), and now is a Professor of Electrical Engineering at *School of Science, Computing and Engineering Technologies*, *Swinburne University of Technology, Australia*. His research interests include battery charging, battery capacity estimation, battery fault diagnosis and battery management systems for electric vehicles and integration of renewable energy sources into power grids.